Optimum Use of V-Blocks for Runout Mesurements

Dr. Axel Rückert, 06.03.2020

1 Introduction

Roundness and flatness are key for shafts of rotating machinery. Runout may be the source of unbalance or can cause rubbing against the stator. Hence radial and axial runout should be checked during the production of a shaft and when the shaft will be repaired.

The ideal situation to check runout would be on a coordinate measuring machine. There the rotor would be stationary in a vertical position and be scanned with a precision sensor system. However when rotors get bigger or measurements need to be performed in the field other measuring systems will be used. All such systems however have systematic measuring errors, which means that the real runout profile of an axial rotor plane differs from the measuring result. One important influence is the way how rotors are being supported during a runout measurement. For example on a lathe a rotor may be held at one end in a chuck and be supported at the other end on a bezel. Another commonly used bearing to perform runout measurements is the V-block. From the literature [1] and [2] we know systems that use several proximity probes to compensate for influences.

This article deals with V-blocks. It will be presented how V-blocks distort the real radial runout profile of an axial rotor plane and how this knowledge can be used for improved runout measurements.

2 Model

The following considerations will be based on the model shown in figure 1. The journal of a rotor is being supported by a V-block with an opening angle 2α. The orientation of the V-block is symmetric to the vertical y-coordinate. The x-ccordinate's orientation is horizontal. The angular coordinate is φ and the journal rotates at the constant angular velocity $\varphi' = \omega$. A measuring gauge or proximity sensor points to the rotor surface under the angle β. I and II are the contact points between the V-block and the journal which are at $\pi + \alpha$ and $-\alpha$ resp..

The runout profile of a rotor is a periodical signal, i.e. it repeats after one revolution. As a result that profile can be developed into a Fourier series, which then describes the

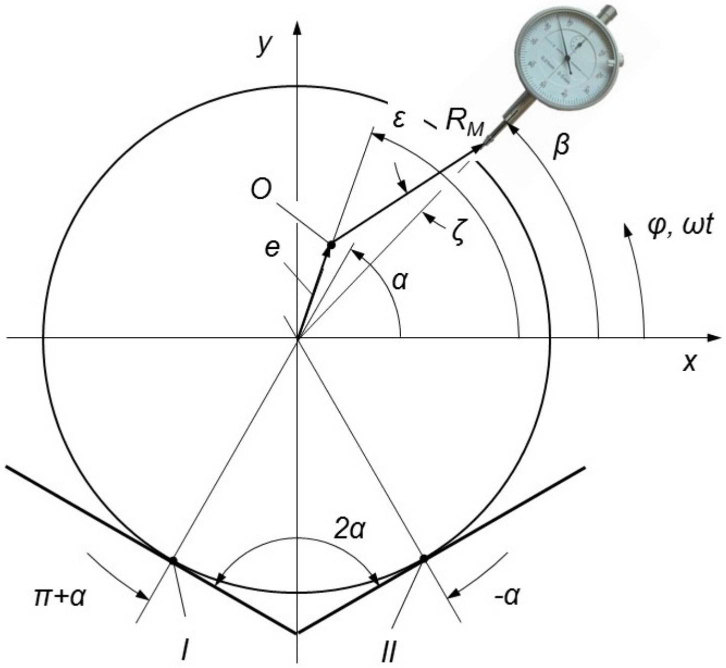

Figure 1: Journal on a V-block

deviation of the shaft radius for the individual orders. As any bearing determines one of the axis points of a shaft the first order component of the Fourier series of a runout profile measured at a bearing is zero per definition. Hence the order of the radius deviations $R^{(n)}(\varphi)$ starts with $n = 2$.

The shaft center O forms the center of the shaft referring to the superimposition of its nominal radius and the first order component of the Fourier series of the runout profile. Due to the runout profile the shaft center moves around with $e(\varphi)$.

3 Measuring Value

The gauge located at the angle β indicates a value which depends on the runout profile and the actual relocation of the journal center:

$$M(\beta, \omega t) = R(\beta - \omega t) \cdot \cos\zeta + e(\omega t) \cdot \cos(\epsilon - \beta) \tag{1}$$

This is actually a projection of R_M and e on the direction with angle β. Applying the sine/cosine addition theorems and the fact that the angle ζ is very small we can rewrite equation (1) to:

$$\begin{aligned} M(\beta, \omega t) &= R(\beta - \omega t) + e(\omega t) \cdot (\cos\epsilon \cdot \cos\beta + \sin\epsilon \cdot \sin\beta) \\ &= R(\beta - \omega t) + e_x(\omega t) \cdot \cos\beta + e_y(\omega t) \cdot \sin\beta \end{aligned} \tag{2}$$

When the gauge was at the positions of the contact points I or II, i.e. $\beta = \pi + \alpha$ or $\beta = -\alpha$ the measuring value was zero, i.e.

$$M(\pi + \alpha, \omega t) = M(-\alpha, \omega t) = 0 \tag{3}$$

Equation (3) now can be used to eliminate the movement of the journal center O. The result is:

$$e_x(\omega t) = \frac{1}{2\cos\alpha}(R(\pi + \alpha - \omega t) - R(-\alpha - \omega t)) \tag{4}$$

$$e_y(\omega t) = \frac{1}{2\sin\alpha}(R(\pi + \alpha - \omega t) + R(-\alpha - \omega t)) \tag{5}$$

Using equations (4) and (5) we can rewrite equation (2) and get a function of the gauge reading which just depends on the unknown runout profile and the measuring parameters α and β:

$$\begin{aligned} M(\omega t) = R(\beta - \omega t) + \frac{1}{2}(\frac{\cos\beta}{\cos\alpha} + \frac{\sin\beta}{\sin\alpha})R(\pi + \alpha - \omega t) \\ - \frac{1}{2}(\frac{\cos\beta}{\cos\alpha} - \frac{\sin\beta}{\sin\alpha})R(-\alpha - \omega t) \end{aligned} \tag{6}$$

As mentioned earlier the runout profile of a rotor is a periodical signal which can be developed into a Fourier series. This means

$$\bar{R}(\varphi) = \sum_{n=2}^{\infty}(\bar{r}^{(n)}e^{in\varphi}). \tag{7}$$

$\bar{R}$ is a complex number which represents a specific runout value at a given angle φ. $\bar{r}^{(n)}$ is a complex number as well and stands for the amount and angle of the n-th order component of a runout profile.

Using equation (7) the gauge reading with equation (6) can also be presented as a Fourier series. The n-th order component of that Fourier series is:

$$\begin{aligned} \bar{m}^{(n)} = \bar{r}^{(n)}e^{in\beta} + \frac{1}{2}(\frac{\cos\beta}{\cos\alpha} + \frac{\sin\beta}{\sin\alpha})\bar{r}^{(n)}e^{in(\pi+\alpha)} \\ - \frac{1}{2}(\frac{\cos\beta}{\cos\alpha} - \frac{\sin\beta}{\sin\alpha})\bar{r}^{(n)}e^{-(in\alpha)} \end{aligned} \tag{8}$$

4 Detection Coefficients

For given angles α and β we can divide equation (8) by $\bar{r}^{(n)}$. We shall call this the n-th order detection coefficient $\bar{d}^{(n)}(\beta)$ of our measuring arrangement:

$$\begin{aligned} \bar{d}^{(n)} = cos(n\beta) + \frac{1}{2}(-1)^n(\frac{\cos\beta}{\cos\alpha} + \frac{\sin\beta}{\sin\alpha})cos(n\alpha) - \frac{1}{2}(\frac{\cos\beta}{\cos\alpha} - \frac{\sin\beta}{\sin\alpha})cos(n\alpha) \\ + i\ (sin(n\beta) + \frac{1}{2}(-1)^n(\frac{\cos\beta}{\cos\alpha} + \frac{\sin\beta}{\sin\alpha})sin(n\alpha) + \frac{1}{2}(\frac{\cos\beta}{\cos\alpha} - \frac{\sin\beta}{\sin\alpha})sin(n\alpha)) \end{aligned} \tag{9}$$

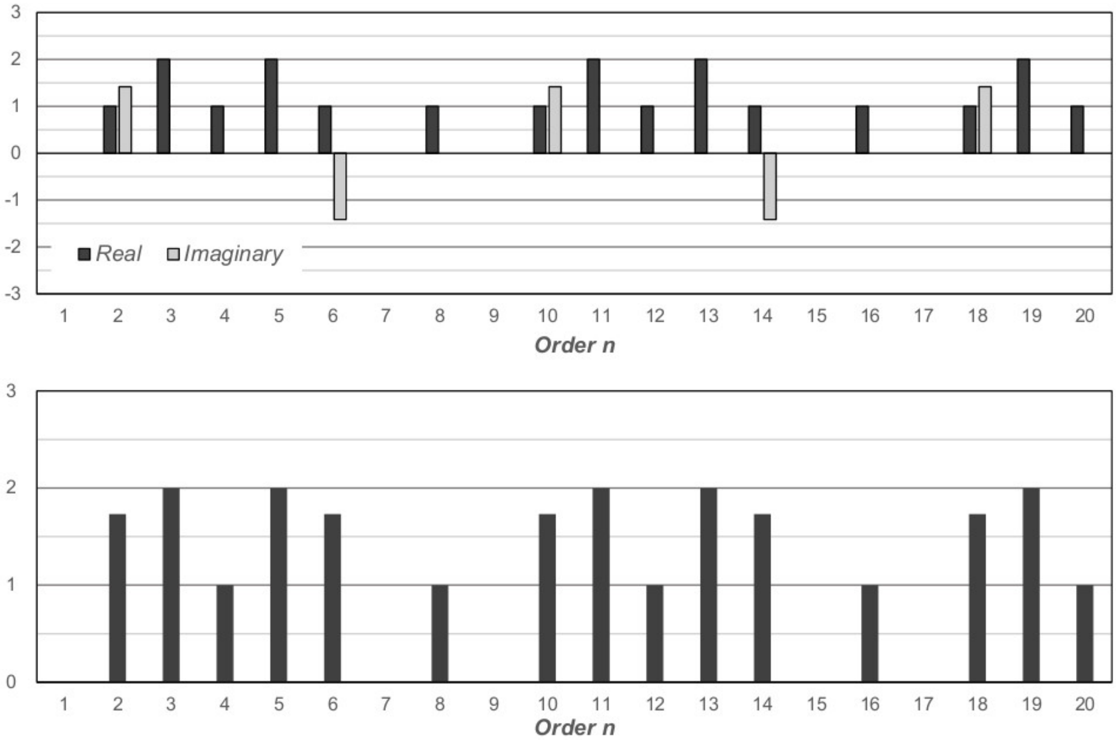

Figure 2: Detection coefficients with $\alpha = 45\ deg.$ and $\beta = 0$ up to an order of 20

Now applying equation (9) let's discuss the influence of different setup parameters β and α on the gauge reading.

In the upper diagram of figure 2 the real and imaginary parts of the detection coefficients for the first 20 orders are shown for a journal on a V-block with opening angle of 90 *deg.* ($\alpha = 45\ deg.$) and $\beta = 0$. The lower diagram shows the amount of the coefficients. The amounts vary with the order at a max. number of 2. For some orders (4, 8, 12, 16 and 20) the coefficient amounts are 1 and for others (7, 9, 15 and 17) the coefficients are zero. For these later orders the movement of the journal center compensates for the runout at the position of the gauge. That means when a runout profile consists of components with these later orders they cannot be detected while other components are being contained in the gauge signal with an amplification of 2.

The diagram in figure 3 shows detection coefficient amounts for various gauge angles β. It appears that a setup with $\beta = 45\ deg.$ is the worst case. Just the even orders will be detected while the uneven orders stay undetected. Gauge angles with $\beta = 0\ deg.$ or 90 *deg.* are better. However still the orders with numbers 7, 9, 15 and 17 will not be detected.

As a conclusion β may be varied to find a setup with a good compromise when all coefficient amounts are greater than zero and the smallest value is in the order of 0.5.

Such a compromise was found for example with $\beta = 85$ *deg.*. From the diagram one can see that all coefficients are different from zero and the amount of the smallest coefficient is about 0.6. Such a setup will result in a measuring signal that contains the individual orders at a high detection rate.

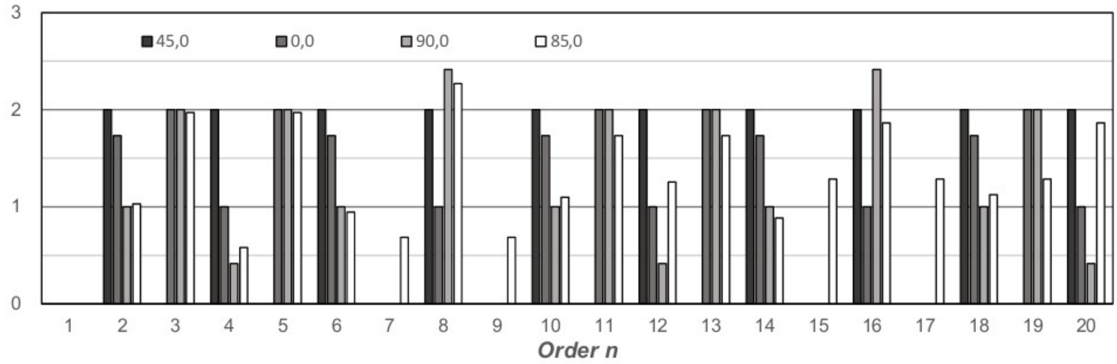

Figure 3: Detection coefficients with $\alpha = 45$ *deg.* and different β-values up to an order of 20

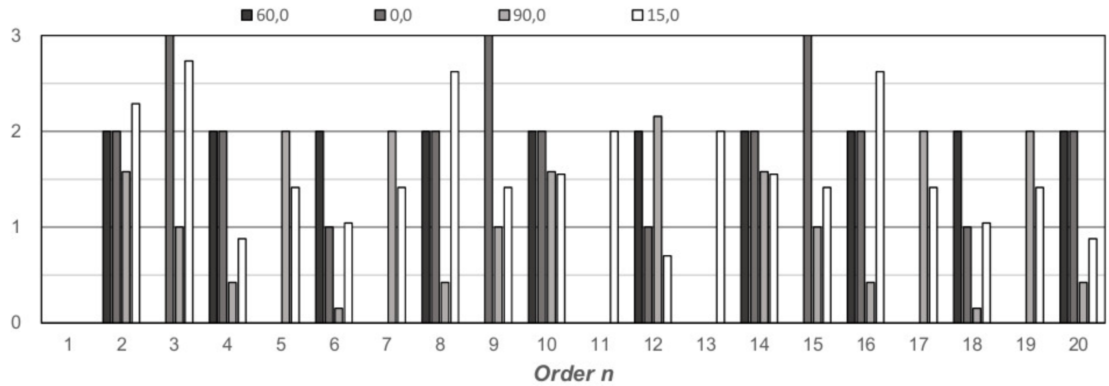

Figure 4: Detection coefficients with $\alpha = 60$ *deg.* and different β-values up to an order of 20

Figure 4 shows the values for a V-block with an opening angle of 120 *deg.* ($\alpha = 60$ *deg.*) and different gauge angles β. The results are similar to the case with $\alpha = 45$ *deg.*. Here a good compromise has been found for an angle $\beta = 15$ *deg.*.

The investigations in this article cover the detection coefficients up to an order of 20. This is already enough to well represent runout profiles of real shafts without scratches.

The equations of this article are also valid for roller bearings. In this case α is the angle between the tangent on the journal's nominal radius at the contact point between journal and roller and the vertical direction. For measuring runout the rollers should have a very small out of roundness condition. The max. permissible runout of a roller

$R_{ro,perm}$ should be smaller than the minimum runout R_{min} which should be measured. As a rule of thumb $R_{ro,perm} < 0.1 \dots 0.2 \cdot R_{min}$.

Another point of concern is the ratio between the radii of the journal and the rollers. In case this ratio is not a natural number it would be sufficient to average the measuring values captured over several revolutions of the journal to eliminate the influence of roller runout.

With runout measurements at shafts with a substantial static sag and an anisotropic bending stiffness it is recommended to arrange the sensor more horizontally. Otherwise the anisotropic bending stiffness would create a phantom second order runout signal, which was the result of the shaft sag due to the different bending stiffnesses.

5 New Runout Measuring Procedure

The above considerations can be applied to runout measurements with journals on V-blocks (or roller bearings) to measure the true runout profile with just one proximity sensor or gauge. This is also called the three-point-method, because we are getting three measuring values at a time - the one from the gauge and the two others from the contact points I and II, where the measuring values are zero.

After the acquisition of measuring data with a given setup (defined by the angles α and β) an order analysis would be performed. Then the detection coefficients will be calculated up to a max. order of the order analysis. Finally dividing the n-th order measuring value component by the n-th order detection coefficient will yield the true runout order component of the journal under examination:

$$\bar{r}^{(n)} = \frac{\bar{m}^{(n)}}{\bar{d}^{(n)}} \tag{10}$$

The true runout profile can now be evaluated by the superimposition of the individual order components up to the max. order under consideration n_{max}:

$$\bar{R}(\varphi) = \sum_{n=2}^{n_{max}} (\bar{r}^{(n)} e^{in\varphi}) \tag{11}$$

With the known runout profile the movement of the journal axis on its support may be calculated using equations (4) and (5). For the n-th order components the result is:

$$\bar{e}_x^{(n)} = \bar{r}^{(n)}(\frac{1}{2\cos\alpha}(e^{in(\pi+\alpha)} - e^{-(in\alpha)})) \tag{12}$$

$$\bar{e}_y^{(n)} = \bar{r}^{(n)}(\frac{1}{2\sin\alpha}(e^{in(\pi+\alpha)} + e^{-(in\alpha)})) \tag{13}$$

The knowledge of the shaft movement is mandatory when the true runout profile of another shaft section adjacent to the one supported on a bearing should be measured. In this case we would use equation (2) to compensate for this movement. For an individual order this yields

$$\bar{p}^{(n)} = (\bar{s}^{(n)} - \bar{e}_x^{(n)} \cos\beta - \bar{e}_y^{(n)} \sin\beta)e^{-(in\beta)}, \tag{14}$$

with p the measuring value and s the component of the runout profile of this other shaft section.

When runout measurements are being performed on long shafts supported by two bearings (V-blocks or rollers) the shaft movements at those bearings may be used to calculate the residual shaft movement at an arbitrary axial rotor plane assuming the shaft can be treated as a rigid body.

6 Practical Validation Measurements

In order to prove and validate the above described method practical measurements have been performed at a model shaft supported on V-blocks, see figure 5.

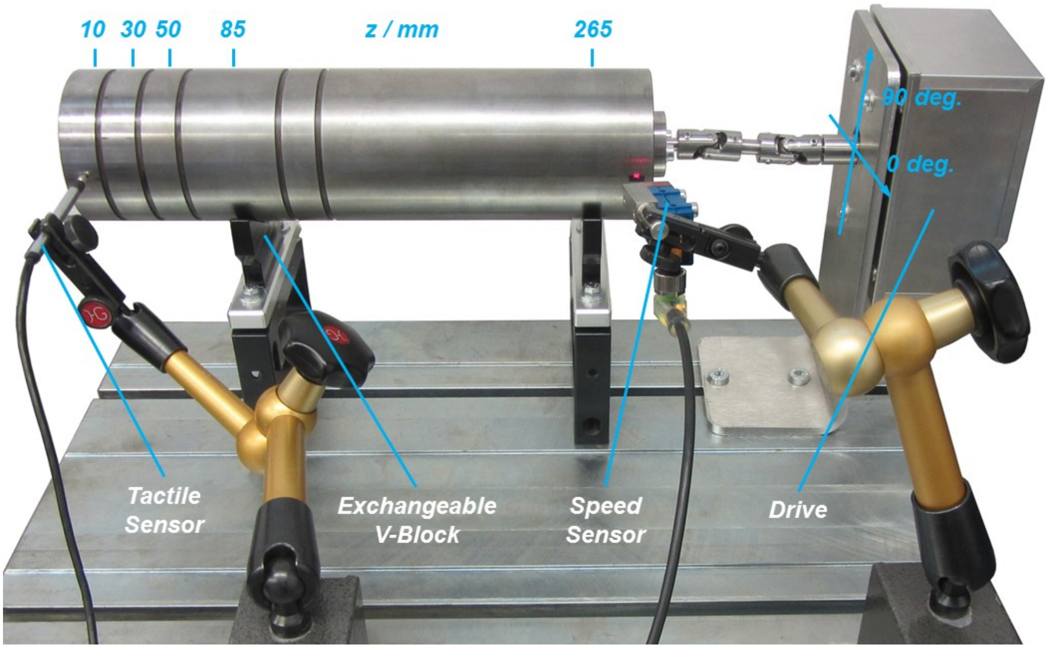

Figure 5: Setup of model shaft on V-blocks

The model shaft has been manufactured from a continuous shaft with a nominal diameter of 80 mm and is 300 mm long. It is supported on pedestals with exchangeable V-blocks and driven from one end by an electric drive at a constant speed of appr. 2.0 1/min. At its other end there are three shaft segments (at axial coordinates $z = 10\ mm$, $30\ mm$ and $50\ mm$ respectively) where an exaggerated runout profile has been introduced by precision grinding. Those profiles mainly show a second, third and fourth order of runout.

Figures 6 and 7 present measuring results (polar diagram and order analysis) from a CMM with the shaft vertical, at the axial planes with the exaggerated runout and at two other axial positions (at $z = 85\ mm$ and $265\ mm$ respectively) where the shaft mainly is cylindrical. While the exaggerated runout is about 20 μm in amplitude, the cylindrical shaft segments show a runout less than about 10 % of that value.

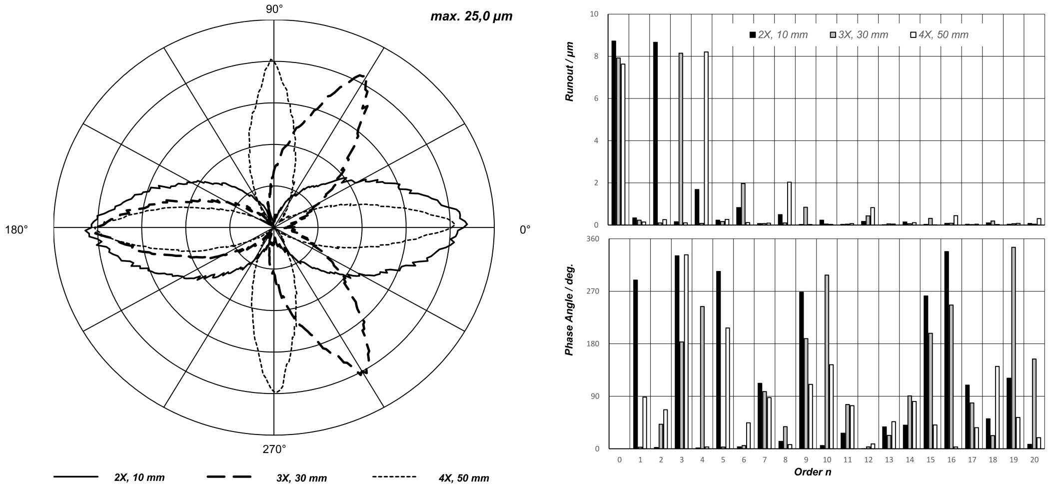

Figure 6: Runout profiles of model shaft measured on CMM at axial positions $z = 10\ mm,\ 30\ mm$ and $50\ mm$

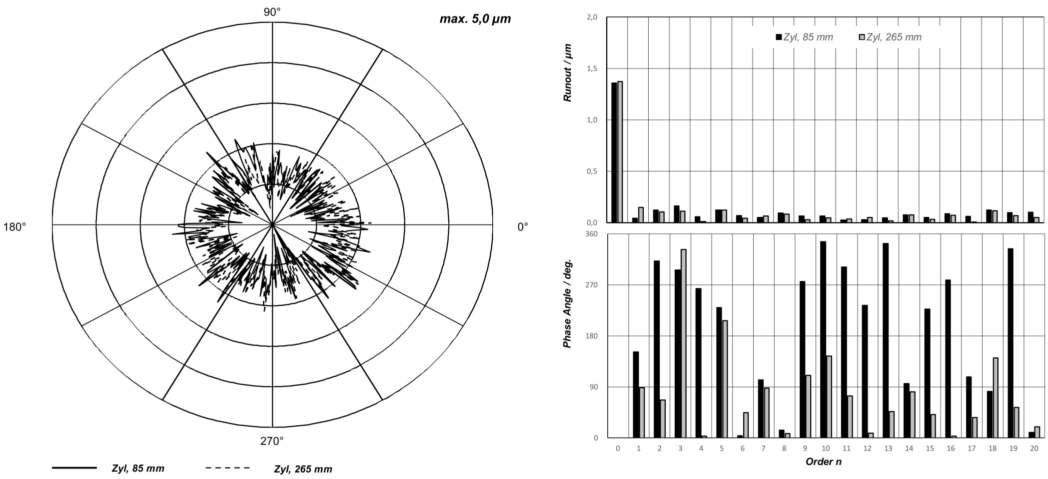

Figure 7: Runout profiles of model shaft measured on CMM at axial positions $z = 85$ mm and $265\ mm$

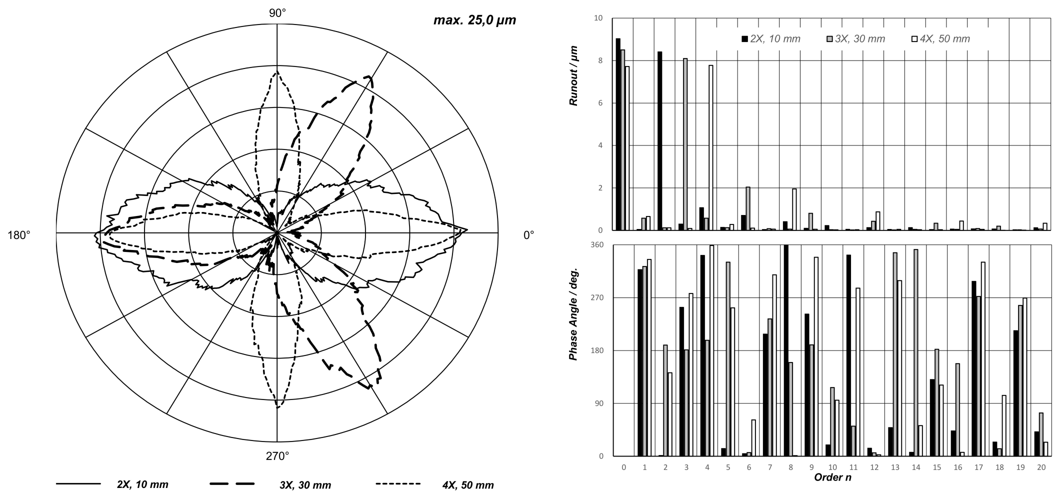

Figure 8: Runout profiles of model shaft measured on V-blocks with $\alpha = 60\ deg.$, $\beta = 0\ deg.$ at axial positions $z = 10\ mm,\ 30\ mm$ and $50\ mm$, supported at $z = 85\ mm$ and $265\ mm$

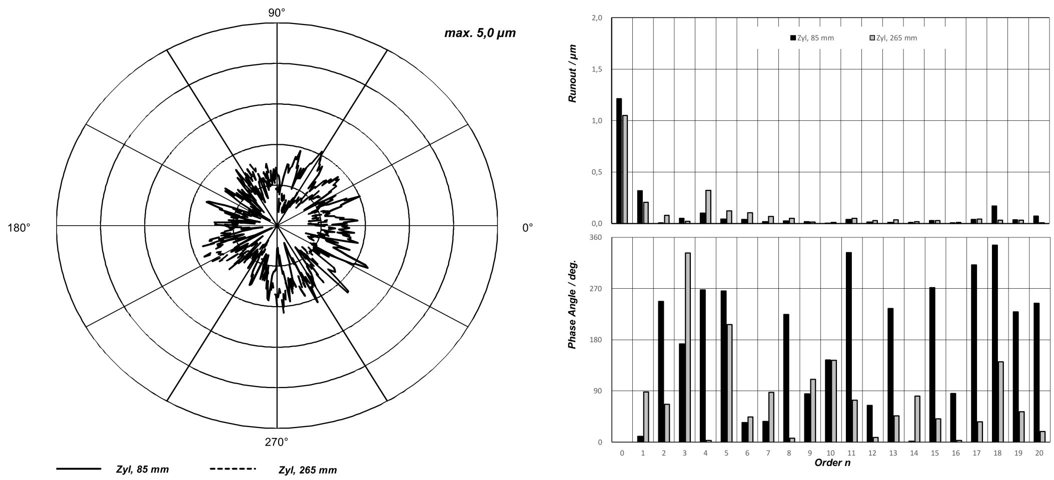

Figure 9: Runout profiles of model shaft measured on V-blocks with $\alpha = 60\ deg.$, $\beta = 0\ deg.$ at axial positions $z = 85\ mm$ and $265\ mm$, supported at $z = 85\ mm$ and $265\ mm$

Then the same measurements have been performed with the shaft setup on V-blocks (similar to figure 5) with 120 $deg.$ opening angle ($\alpha = 60\ deg.$) at $z = 85\ mm$ and 265 mm with a tactile measuring sensor at $\beta = 0\ deg.$. The polar diagrams in figures 8 and 9 display the results which are very similar to the CMM. Reason is that the runout at the V-block supports is less than 10 % of the runout at the three planes with exaggerated runout. This yields almost no shaft axis movement at the support positions which might destort the runout profile.

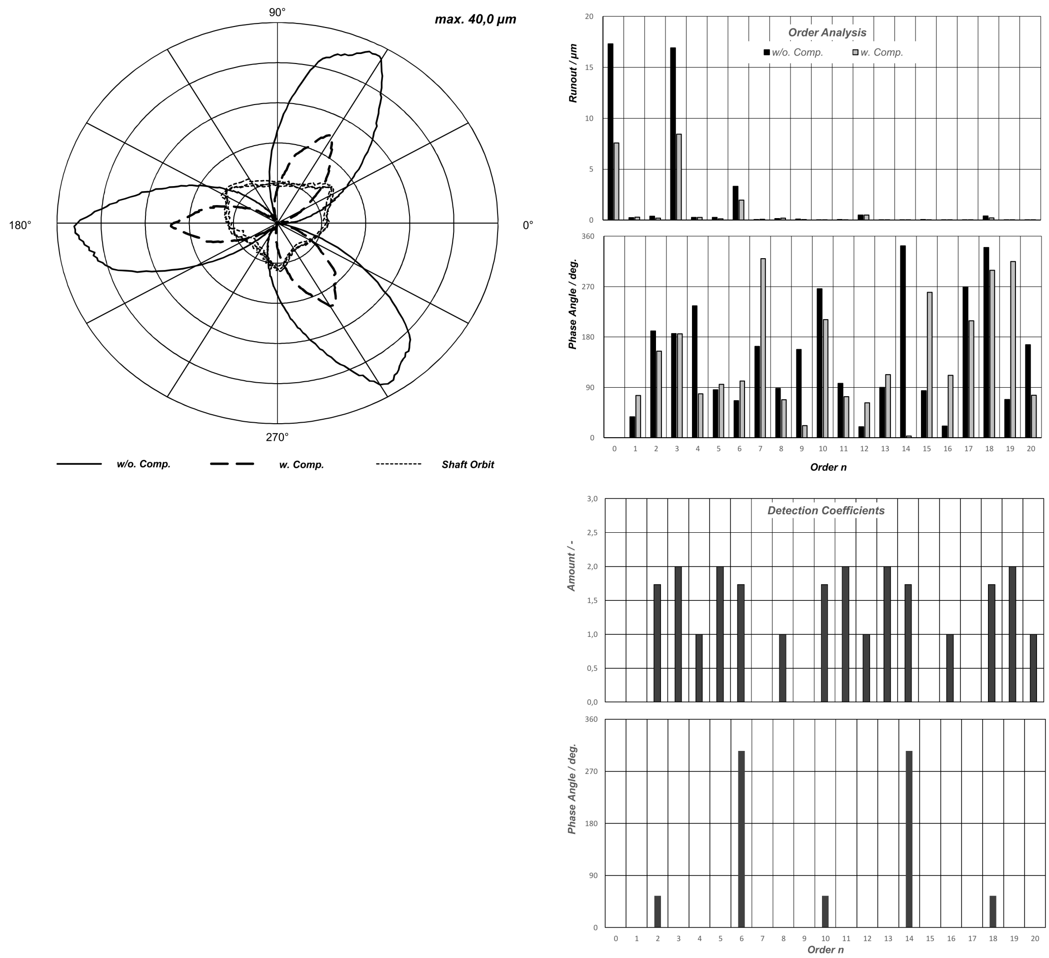

Figure 10: Raw and compensated runout profile and shaft orbit for $z = 30\ mm$, support at $z = 30$ and 265 mm, $\alpha = 45\ deg.$, $\beta = 0\ deg.$

With the next measurements the model shaft has been supported on 90 $deg.$ V-blocks ($\alpha = 45\ deg.$) at $z = 30\ mm$ (exaggerated third order runout) and 265 mm (mainly cylindrical) respectively. The diagrams of figures 10 and 11 now show for different measuring angles β how the real runout profile of the shaft at $z = 30\ mm$ is distorted by the movement of the shaft axis on the V-block introduced by the shaft runout itself. The

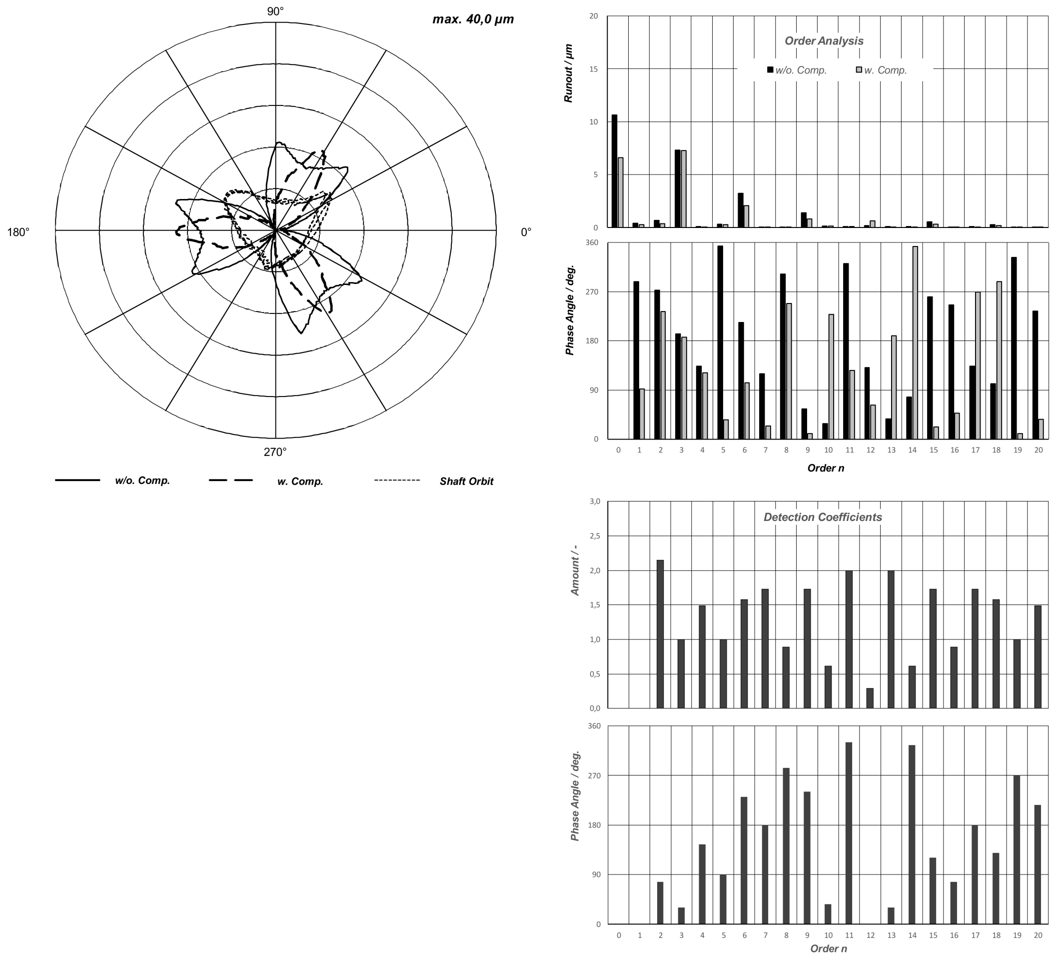

Figure 11: Raw and compensated runout profile and shaft orbit for $z = 30$ mm, support at $z = 30$ and 265 mm, $\alpha = 45$ $deg.$, $\beta = 30$ $deg.$

diagrams contain the polar presentation of the runout profile, the shaft axis movement, the order analysis and the detection coefficients (for the first twenty orders). Finally also the runout profile compensated by the detection coefficients is presented, which is well in accordance with the measurements on the CMM and with the shaft supported on cylindrical journals.

However with a measuring angle $\beta = 45\ deg.$ the real runout profile cannot be measured (figure 12). This is because all the uneven detection coefficients for a V-block with 90 deg. ($\alpha = 45$ deg.) and a measuring angle of $\beta = 45$ deg. are zero (see also figure 2). In this case just the even orders of the runout can be evaluated, which can be seen for orders 6 and 12.

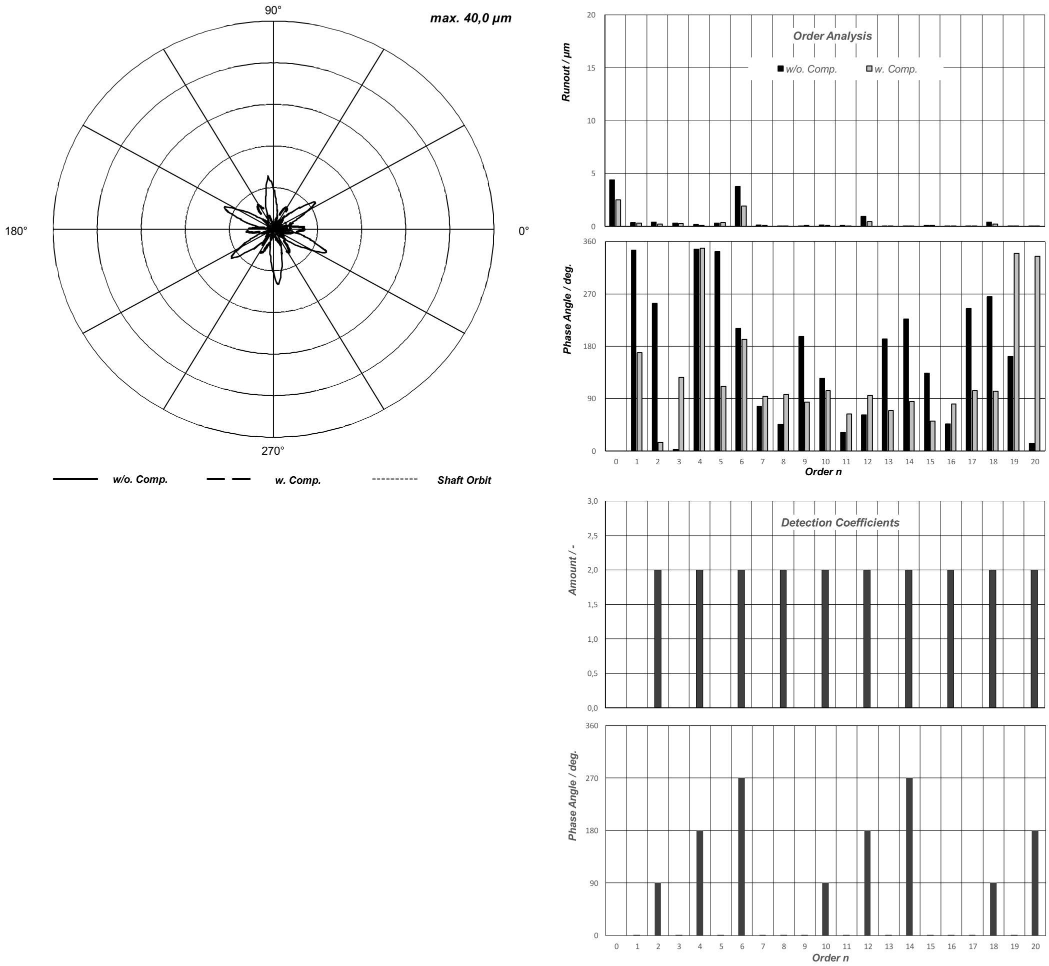

Figure 12: Raw and compensated runout profile and shaft orbit for $z = 30\ mm$, support at $z = 30$ and $265\ mm$, $\alpha = 45\ deg.$, $\beta = 45\ deg.$

Finally the model shaft has been supported again on 120 *deg.* V-blocks ($\alpha = 60\ deg.$)

at $z = 30\ mm$ (exaggerated third order runout) and $265\ mm$ (mainly cylindrical) respectively with the tactile measuring sensor at $\beta = 0\ deg.$. First the runout profiles at the support locations have been measured and compensated with the detection coefficients of the three-point-method. Then the exaggerated runouts with mainly second order at $z = 10\ mm$ and fourth order at $z = 50\ mm$ have been measured which shows quite a distortion of the runout profiles by the shaft movement on the V-blocks (figure 13). To compensate for the shaft movement it is assumed that the shaft axis forms a straight line. Then the shaft movements evaluated at the support locations can be used to calculate the radial shaft movement at any other axial location. Applying this with the measurement values for $z = 10\ mm$ and $z = 50\ mm$ almost yields the real runout profile as measured on the CMM.

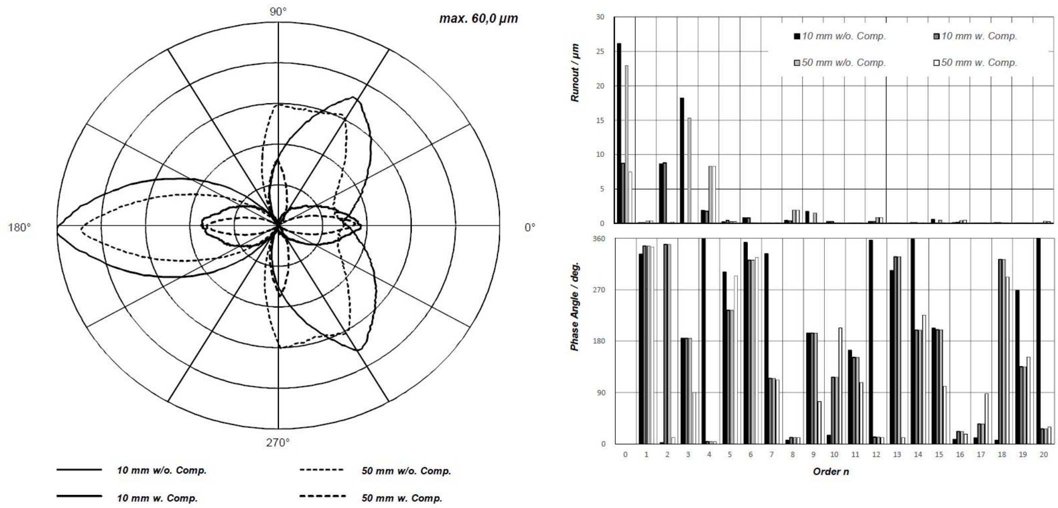

Figure 13: Raw and compensated runout profiles for $z = 10$ and $50\ mm$, support at $z = 30$ and $265\ mm$, $\alpha = 60\ deg.$, $\beta = 0\ deg.$

7 Conclusion

With this article a runout measuring procedure was introduced which implements measuring error compensation. The raw measuring values captured at a journal on a V-block or roller bearing with one single sensor will not represent the true runout profile of a journal. This is because the movement of the journal axis is part of the measuring signal. The considerations are based on the fact that a runout profile is a periodic signal and can be developed into a Fourier series. For a given measuring setup (opening angle of contact points and measuring angle) there are detection coefficients which translate the true runout profile to a measuring signal. These detection coefficients can be used to compensate for the movement of the journal axis. Furthermore those coefficients tell what order of a runout profile can be measured with a given setup.

Once the true runout profile has been determined also the movement of the journal axis can be calculated. This is useful when runout measurements should be performed at other axial shaft sections where is no support.

Finally the validation of the described method has been presented with runout measurements at a model shaft on V-blocks.

The new runout measuring method is available with the portable Runout Testing System RO 7000 and the stationary Runout Testing Machines Type UHR from Hofmann.

References

[1] S. Adamczak, D. Janecki, and K. Stepien. “Cylindricity measurement by the V-block method – theoretical and practical problems.” In: *Measurement* 44.1 (2011), pp. 164–173.

[2] B. Muralikrishnana et al. “A note on the three-point method for roundness measurement.” In: *Precision Engineering* 29 (2005), pp. 257–260.